OCEANOGRAPHY

# Dimorphism in cryptophytes—The case of *Teleaulax amphioxeia*/*Plagioselmis prolonga* and its ecological implications

**A. Altenburger[1]*†, H. E. Blossom[2], L. Garcia-Cuetos[3], H. H. Jakobsen[4], J. Carstensen[4], N. Lundholm[3], P. J. Hansen[5], Ø. Moestrup[6], L. Haraguchi[4]*†‡**



**Growing evidence suggests that sexual reproduction might be common in unicellular organisms, but observations are sparse. Limited knowledge of sexual reproduction constrains understanding of protist ecology. Although *Teleaulax amphioxeia* and *Plagioselmis prolonga* are common marine cryptophytes worldwide, and are also important plastid donors for some kleptoplastic ciliates and dinoflagellates, the ecology and development of these protists are poorly known. We demonstrate that *P. prolonga* is the haploid form of the diploid *T. amphioxeia* and describe the seasonal dynamics of these two life stages. The diploid *T. amphioxeia* dominates during periods of high dissolved inorganic nitrogen (DIN) and low irradiance, temperature, and grazing (winter and early spring), whereas the haploid *P. prolonga* becomes more abundant during the summer, when DIN is low and irradiance, temperature, and grazing are high. Dimorphic sexual life cycles might explain the success of this species by fostering high genetic diversity and enabling endurance in adverse conditions.**

## INTRODUCTION

Cryptophytes are important unicellular primary producers and ubiquitous components of plankton assemblages. Cryptophytes are nontoxic and considered good quality food for other protists. Their small size, varying between 4 and 50 μm, puts them at the base of the food web, consumed by a wide variety of organisms. Knowledge of the relative importance of cryptophytes within marine phytoplankton communities is still scarce. This knowledge gap has persisted because of difficulties in identifying cryptophytes to species level by light microscopy and because the delicacy of their cell structures makes it difficult to fix these cells with standard methods (*1*). It is well established , however, that some cryptophytes are important plastid donors for kleptoplastidic dinoflagellates and ciliates in the plankton (*2*).

The cryptophyte *Teleaulax amphioxeia* occurs worldwide and serves as plastid donor to the ciliates *Mesodinium major* and *Mesodinium rubrum* (*3*). Very little is known about *M. major*, but *M. rubrum* is an important food source and a plastid donor for the dinoflagellates *Amylax triacantha* and *Amylax buxus* (*4*, *5*) and at least six species of *Dinophysis* [reviewed in (*6*)]. The cryptophyte species *T. amphioxeia* is a particularly important food source in nature, as investigations on natural populations have shown that chloroplasts found in *M. rubrum* (*7*) and *Dinophysis acuminata* (*8*) were predominantly from *T. amphioxeia*. It has been demonstrated that the cosmopolitan *M. rubrum* can use chloroplasts from different species of *Teleaulax* but are unable to use chloroplasts from other cryptophyte genera (*3*, *7*). Thus, the coupling of taxonomy and ecology is essential to gain a better understanding of the role of cryptophytes in aquatic ecosystems.

Traditionally, cryptophyte systematics has been based on biliprotein types and various morphological traits, such as position of the nucleomorph, ultrastructural characteristics of the flagellar root apparatus, variations in the furrow/gullet complex, the inner periplast component (IPC; consisting of either polygonal plates or a continuous sheet), and the surface periplast component (SPC) (*9*). Following advances in molecular tools, recent research has revealed that biliprotein type seems to be congruent with molecular phylogenies, but the traditionally definitive morphological trait of IPC structure is not, thus reducing its taxonomic importance (*10*). In molecular studies on cryptophytes, several clades consisting of species complexes stand out as not congruent with their morphological, ultrastructural characteristics, such as *Chroomonas*/*Komma*, *Rhodomonas*/*Rhinomonas*/*Storeatula*, *Guillardia theta*/*Hanusia phi*, and *Geminigera*/*Plagioselmis*/*Teleaulax* (*11*).

An increasing number of phytoplankton species, including cryptophytes, are reported to have complex life cycles that involve more than one morphotype, and in some cases, they have previously been identified as different species (*12*, *13*). *Proteomonas sulcata* was the first example of a cryptophyte species in which a dimorphic life cycle was described, and the two forms can be distinguished by size, periplast structure, the configuration of the flagellar apparatus, and the quantity of nuclear DNA (*12*). Previously established cryptophyte genera have also been suggested to be part of a potential dimorphic life cycle as *Campylomonas* and *Cryptomonas*, which have identical 18*S* ribosomal DNA (rDNA) sequences but differ by having a sheet-like or a plated periplast, respectively (*14*). Whether or not these two forms also represent haploid and diploid stages of the life cycle is unknown. The authors called the form with plated periplast "cryptomorph" and the one with sheet-like periplast "campylomorph" (*14*). On the basis of similarities in DNA sequences, it has been suggested that dimorphism could be a common trait among the cryptophytes (*10*) and that each species has a form with plated periplast

[1]The Arctic University Museum of Norway, UiT–The Arctic University of Norway, 9006 Tromsø, Norway. [2]Aquatic Ecology Unit, Department of Biology, Lund University, Sölvegatan 37, 22362 Lund, Sweden. [3]Natural History Museum of Denmark, University of Copenhagen, Gothersgade 130, 1123 Copenhagen, Denmark. [4]Department of Bioscience, Aarhus University, Frederiksborgvej 399, 4000 Roskilde, Denmark. [5]Marine Biological Section, University of Copenhagen, Strandpromenaden 5, 3000 Helsingør, Denmark. [6]Marine Biological Section, University of Copenhagen, Universitetsparken 4, 2100 Copenhagen Ø, Denmark.
*Corresponding author. Email: andreas.altenburger@uit.no (A.A.); lumi.haraguchi@ymparisto.fi (L.H.)
†These authors contributed equally to this work.
‡Present address: Marine Research Centre, Finnish Environment Institute (SYKE), 00790 Helsinki, Finland.

and an alternate form with sheet-like periplast. Therefore, dimorphism provides a potential explanation for the incongruence of the periplast structure of cryptophytes in molecular phylogenies found in and among different studies (*15*). A description of life cycle stages should hence involve investigations of ploidy and a careful taxonomical review in addition to the comparison of DNA sequences, especially when two formerly distinct genera are involved. Ecological aspects of the dimorphic life cycles remain understudied, limiting our interpretation of the significance of those strategies in nature.

This is the first study that links dimorphic life cycles and ecology in cryptophytes. We found a significant correlation between the distribution of two species and dissolved inorganic nitrogen (DIN) in environmental samples. It turned out that these species were two life cycle stages of the same species. Life cycle stage changes were observed in cultures under constant light and temperature regime. To elucidate the long-suspected dimorphism of *T. amphioxeia* and *Plagioselmis prolonga* (*14*, *16*) and its ecological implications we (i) assessed potential dimorphism by analyzing a time series of the abundance of these cryptophytes in a temperate mesohaline shallow estuary (Roskilde Fjord, Denmark), (ii) investigated similarities in the 18*S* rDNA of species in the *Plagioselmis*/*Teleaulax*/*Geminigera* clade, (iii) investigated the occurrence of nuclear phase changes by comparing the amount of DNA in *P. prolonga* and *T. amphioxeia*, and (iv) compared the morphology of *P. prolonga* and *T. amphioxeia* using scanning electron and light microscopy to address the taxonomic revision of the two species.

## RESULTS

### In situ dynamics

Overall, the two populations, *P. prolonga* and *T. amphioxeia*, co-occurred and displayed similar seasonal dynamics in Roskilde Fjord (Fig. 1A). Both populations were present in all observations, with the highest abundances in March (early spring) in both years (Fig. 1A). The lowest abundances were observed in June to July 2016 and April to May 2017 (Fig. 1A). During winter and early spring, the abundance of *T. amphioxeia* was higher than *P. prolonga* (Fig. 1A). For the rest of the year, the cell numbers of the two populations were similar but with higher cell numbers of *P. prolonga* compared to *T. amphioxeia* in May to October 2016, April to May 2017, and July to August 2017 (Fig. 1A).

During spring, inorganic nutrients (both nitrogen and phosphorus) are depleted simultaneously (Fig. 1B). DIN and the ratio between cell abundances of *P. prolonga* and *T. amphioxeia* ($R_{crypto}$) exhibited almost inverse patterns as the ratio increased with decreasing DIN and vice versa (Fig. 1B). This was not observed for dissolved inorganic phosphorus (DIP) (Fig. 1B and fig. S1). The generalized additive model (GAM) analysis revealed a significant linear relationship with DIN ($P < 0.0001$) and significant time departures ($P < 0.0001$) from this relationship (Fig. 1, C and D). The time trajectories generally followed the DIN relationship with idiosyncratic departures typically lasting 1 to 2 months. The estimated relationship to DIN indicated that *P. prolonga* on average would be more abundant than *T. amphioxeia* when DIN is <1.6 μM.

### Phylogeny

The genera *Teleaulax*, *Plagioselmis*, and *Geminigera* form one clade with maximum support in the phylogenetic analysis (Fig. 2 and fig. S2). A sister group to this clade is formed by *H. phi* and *G. theta*. Within the *Teleaulax*/*Plagioselmis*/*Geminigera* clade, *T. amphioxeia* clusters with *P. prolonga*, supporting the hypothesis that these are different life cycle stages of the same species. Sister group to *T. amphioxeia* is *Teleaulax acuta*. *Geminigera cryophila* clusters together with *Plagioselmis nannoplanctica*. *Teleaulax gracilis* and *Teleaulax minuta* are also part of this clade.

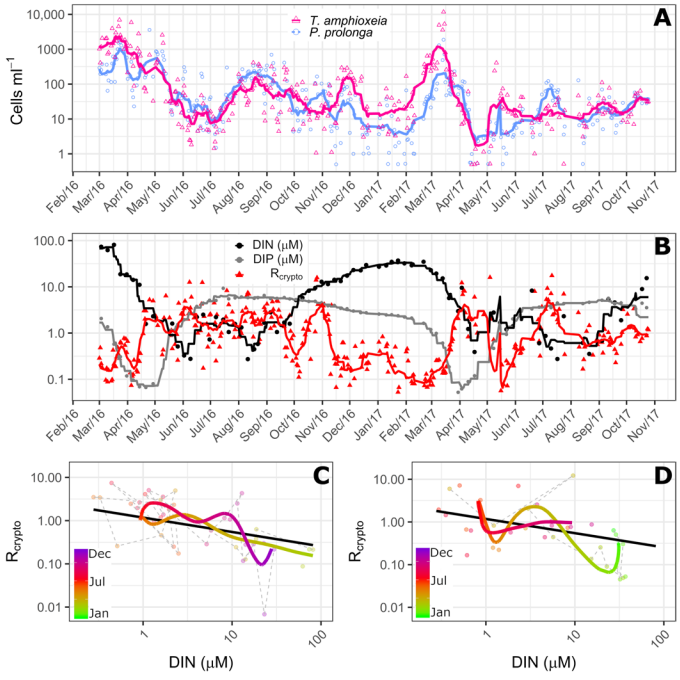


**Fig. 1. Dynamics of *Plagioselmis prolonga* and *Teleaulax amphioxeia*.** (**A**) Dynamics of cell abundance of *P. prolonga* (blue circles) and *T. amphioxeia* (pink triangles) in Roskilde Fjord from March 2016 to November 2017. (**B**) Dynamics of $R_{crypto}$, the ratio between *P. prolonga* to *T. amphioxeia* (red triangles), DIN (black circles), and DIP (gray circles) concentration for the same period depicted in (A). (**C** and **D**) Trajectory dynamics between $R_{crypto}$ and DIN concentrations in 2016 (C) and 2017 (D). In (A) and (B), symbols are the observations, and lines are the 10 days moving average. In (C) and (D), dots represent the observations, colored thick lines represent the time trajectories estimated from the GAM, and the thick black lines represent the linear relationship between DIN and $R_{crypto}$. Trajectories for the 2 years are shown separately for better visualizing the idiosyncrasy.

### Ploidy

*P. prolonga* cultures were denser than *T. amphioxeia*, as reflected by the higher nuclei counts (Fig. 3). Optical profiles of *P. prolonga* were characterized by a fluorescence peak of 885 ± 114 mV (means ± SD, $n = 479$) and total fluorescence of 8888 ± 810 mV, whereas *T. amphioxeia* nuclei profiles exhibited a fluorescence peak of 1700 ± 248 mV ($n = 176$) and total fluorescence of 18475 ± 1703 mV. The total fluorescence of *T. amphioxeia* nuclei is 2.08 times the mean total fluorescence found in *P. prolonga* nuclei (Fig. 3), supporting the hypothesis that *P. prolonga* is haploid and *T. amphioxeia* is diploid.

### Morphology

Color variation has been observed in cells of both the diploid and haploid forms, with live cells varying from reddish brown to olive green (Figs. 4, A and B, and 5, A and B). Cell shape varies from elongated to more rounded (Figs. 4, A and B, and 5, A and B). During exponential growth, the elongated and reddish cells are most prominent,

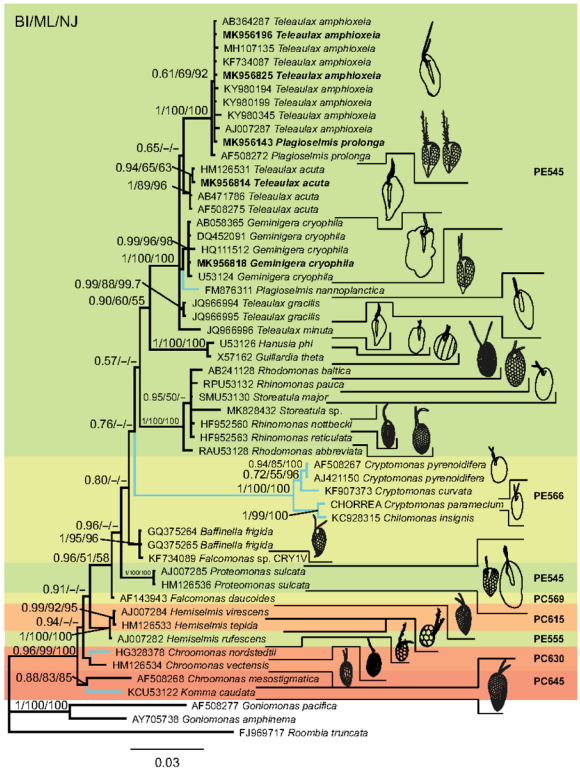


**Fig. 2. Phylogeny of cryptophytes analyzed by Bayesian inference of 18*S* rDNA sequences.** Numbers at nodes represent the posterior probability of Bayesian analysis/bootstrap values of maximum likelihood out of 1000 replicates/bootstrap values of neighbor-joining out of 10,000 replicates. Not resolved branches and branches with support values below 50% are marked with a minus sign (–). The scale bar corresponds to three substitutions per 100 nucleotide positions. Colors correspond to absorption maxima (i.e., PE545 = green). Branches for freshwater species are blue, marine and brackish species are black. Newly sequenced strains are in bold. Drawings of cells are not to scale.

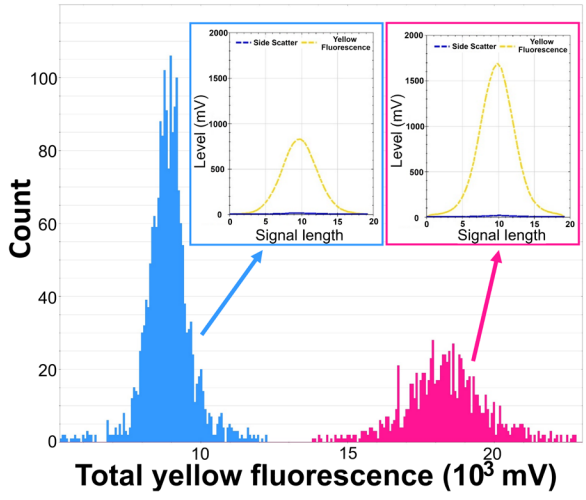


**Fig. 3. Nuclei fluorescence of *P. prolonga* and *T. amphioxeia*.** Histograms showing the nuclei counts in different classes of total yellow fluorescence (FLY) (proxy for amount of DNA) in extracted nuclei of *P. prolonga* (blue) and *T. amphioxeia* (pink) cultures stained with SYBR green dye. An example of an optical profile for the nuclei of each species is also provided, showing the high FLY and low SWS signal (characteristic for the nuclei) and differences in the FLY intensity between the two forms.

whereas more rounded cells and, occasionally, the greenish color appear during stationary phase.

Cells of the haploid *P. prolonga* stage are 6 to 8 µm long and 3 to 5 µm wide (Fig. 4, D and E). Two cell types could be found within the cultures, both having an acute antapical end. In one cell type, the antapical end is more elongated, resembling a tail (Fig. 4, A, C, and D), while in the other, the antapical end is shorter (Fig. 4, B, C, and E). All cells bear a prominent ventral furrow (Fig. 4F). The two flagella are inserted in a cavity at the right side of the apical end of the furrow (Fig. 4F), the dorsal flagellum being longer than the ventral. The cell surface is covered by pentagonal or—more commonly—hexagonal plates and cover the entire cell surface apart from the antapical end, which lacks plates (Fig. 4, G and H). The surface of the antapical end is somewhat uneven, with small knobs that indicate ejectosome openings (Fig. 4H). Small extrusomes are released from the narrow "sutures" between the plates, often at a junction of three plates. Holes in the sides of the furrow probably mark points where large ejectosomes have been discharged (Fig. 4F). The periplast plates are generally slightly smaller along the furrow, the flagellar insertion, and anteriorly. The plates appear to be arranged on the right-hand side in five to six irregular, oblique horizontal rows (Fig. 4E). On the left-hand side of the cell, the plates extend over the cell apex without being interrupted by the flagellar canal, in seven to eight rows. A prominent longitudinal band extends from the region of the antapical end of the furrow to the cell antapex [the so-called mid-ventral band of Hill and Wetherbee (*12*)], typically about 4 µm in length. The mid-ventral band often terminates a short distance before the furrow (Fig. 4H); in other cells, it extends for a very short distance along the left side of the furrow, and in other cells again, the band dichotomizes at the base of the furrow and extends for a short distance along the two sides of the furrow (Fig. 4G). It also extends onto the dorsal side but only for about 1 µm (Fig. 4I).

The diploid *T. amphioxeia* stage is very different. The cells are 8 to 13 µm long and 4 to 6 µm wide (Fig. 5, D and E). The flagella insert near the anterior end of the right-hand side of the furrow as in the *Plagioselmis* stage. The two flagella, however, show reversed relative lengths, the ventral flagellum being longer than the dorsal (Fig. 5G). The inner periplast is a sheet-like periplast and does not show any sign of plates. The surface periplast is papillate. The only other feature of the *Teleaulax* stage that deserves mentioning is the presence of a short, curved, mid-ventral band (Fig. 5H). In *Teleaulax*, in contrast to the *Plagioselmis* stage, the mid-ventral band passes in an oblique direction from the antapex and measures only ca. 2.5 µm in length. In short, the two stages of the life cycle differ in size, relative flagellar length, periplast structure, and in the paths and lengths of the mid-ventral band (for a summary, see table S1).

## DISCUSSION

The taxa *P. prolonga* and *T. amphioxeia* represent different life stages of the same species. This conclusion is based on our observations on laboratory-grown cultures, congruence of 18*S* rDNA sequences, and different ploidy of the two taxa. We provide evidence that *P. prolonga* is the haploid stage and *T. amphioxeia* the diploid stage of the same life cycle, and most importantly, that these two stages show distinct ecological preferences.

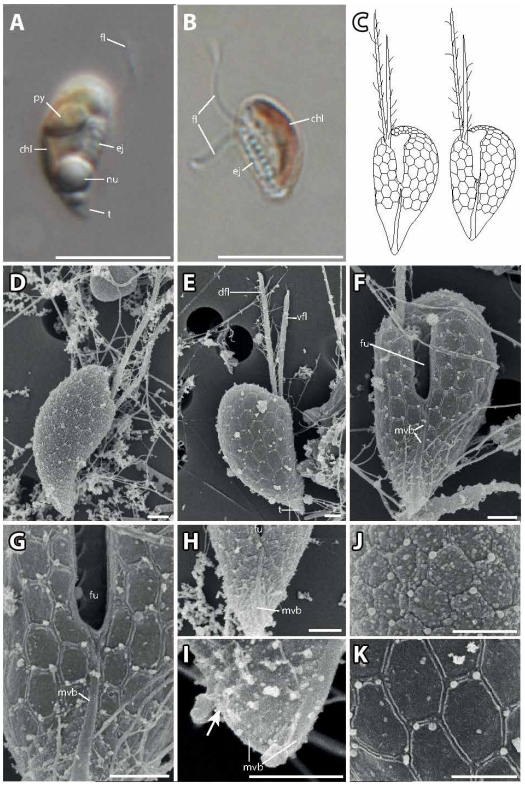


**Fig. 4. *P. prolonga* morphology.** (**A**) Lateral view of *P. prolonga* with the tail (t), nucleus (nu), ejectosomes (ej), pyrenoid (py), and flagellum (fl). (**B**) Lateral view of *P. prolonga* without the tail, with chloroplast (chl), ejectosomes, and flagella. (**C**) Drawings of *P. prolonga* cell with the tail (left) and without the tail (right). (**D**) Lateral view with part of the surface periplast component (SPC). (**E**) Lateral view showing the inner periplast component (IPC) and tail; note the hexagonal periplast plates of the IPC and the ventral flagellum (vfl), which is shorter than the dorsal flagellum (dfl). (**F**) Ventral view of a cell without tail. The furrow (fu), IPC, flagella, and the mid-ventral band (mvb) are visible. (**G**) Closeup of (C) with detail of the mid-ventral band that bifurcates at the base of the furrow. (**H**) The mid-ventral band terminates before reaching the furrow and does not bifurcate. (**I**) Detail of the posterior end of a cell without tail. There are no hexagonal plates at the posterior end, and the mid-ventral band extends onto the dorsal side of the cell (arrow). (**J**) Detailed view of the periplast; the particles are probably part of the SPC. (**K**) Detailed view of the IPC. Scale bars are 10 μm (light microscopy) and 1 μm [scanning electron microscopy (SEM)]. Anterior of all cell oriented upwards.

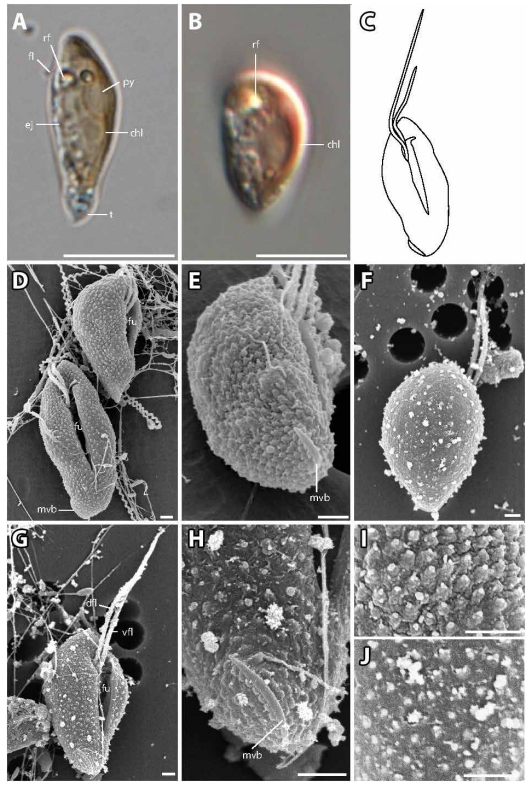


**Fig. 5. *T. amphioxeia* morphology.** (**A**) Lateral view of elongated *T. amphioxeia* cell with olive-brown color with chloroplast, refractosome (rf), pyrenoid, and ejectosomes. (**B**) Lateral view of a more round *T. amphioxeia* cell, more reddish in color with chloroplast and refractosome. (**C**) Drawing of *T. amphioxeia* surface characters. (**D**) Ventral and lateral view of cells with intact SPC with a papillate structure (fixation with Lugol's solution), furrow, and mid-ventral band that is almost lateral at the antapical end. (**E**) View from lateroposterior on the cell with SPC showing the short mid-ventral band. (**F**) Dorsal view of the cell with sheet-like IPC (fixation with $OsO_4$). (**G**) Ventral view showing the furrow and ventral flagellum that is longer than the dorsal flagellum. (**H**) Detail of the antapical end with the mid-ventral band, which is short and curved and does not extend to the furrow. (**I**) Detail of the cell surface SPC visible in fixation with Lugol's solution. (**J**) Detail of the cell surface IPC in fixation with $OsO_4$. Scale bars are 10 μm (light microscopy) and 1 μm (SEM). Anterior of all cell oriented upwards.

## Taxonomic considerations

The genus *Plagioselmis* was originally described by Butcher in 1967 (*17*) to comprise two species. His description was not valid, as he failed to designate one of the species as type [International Code of Nomenclature for algae, fungi, and plants; ICN, Shenzhen Code, Art. 7 (*18*)]. In 1990, Chrétiennot-Dinet (*19*) designated *P. prolonga* as type species but failed to give a full reference to Butcher's description, and her designation is therefore also invalid (ICN. Art. 41.5). The first valid description of the *Plagioselmis* genus was in 1994 by Novarino *et al.* (*20*), who provided a discussion of the species known at the time.

*Teleaulax* was described in 1991 by Hill (*21*) with *T. acuta* as type species. This generic name is, therefore, older than the first valid publication of the genus *Plagioselmis* from 1994. After finding that *P. prolonga* is the haploid stage of the life cycle of *T. amphioxeia*, the correct name for the species is *T. amphioxeia*, and *P. prolonga* is a synonym. *T. amphioxeia* is thus composed of two morphotypes, the diploid stage (*T. amphioxeia*) and the haploid stage, which we suggest calling the *Plagioselmis* stage of *T. amphioxeia*.

## Dimorphism in the cryptophytes

Hill and Wetherbee (*12*) were the first to show, in *P. sulcata*, a cryptomonad life cycle comprising two morphologically different stages. One morphotype was larger (9 to 14 μm), with a sheet-like periplast, and the other was slightly smaller (7.5 to 10.5 μm), with a periplast consisting of hexagonal plates. The DNA content of the larger morphotype was twice that of the smaller morphotype, indicating that the two morphotypes, one diploid and one haploid, were different life stages of a complex life history.

On the basis of identical molecular sequences, Hoef-Emden *et al.* (*14*) found another dimorphism in species of what used to be considered two separate genera, *Cryptomonas* and *Campylomonas*. Like the two morphotypes of *P. sulcata*, the authors found that one

morphotype had an IPC consisting of hexagonal plates (*Cryptomonas*-like, termed cryptomorph), while the other had a sheet-like IPC (*Campylomonas*-like, termed campylomorph). Although not investigated, it is likely that the two morphotypes of the same species also involve a nuclear phase change.

Here, we provide a third example of a true dimorphism in the cryptomonads. Similar to both *P. sulcata* and the species in the genus *Cryptomonas*, one morphotype of *T. amphioxeia* is larger with a sheet-like IPC, and the other is smaller with an IPC consisting of hexagonal plates (Figs. 4 and 5). Consistent with the case of *P. sulcata*, the larger stage has twice the DNA of the smaller stage (Fig. 3) and is thus the diploid morphotype, and the smaller is the haploid "*Plagioselmis* stage."

Recently, another cryptophyte with a suspected dimorphism (*Baffinella frigida*) was described from the Arctic by Daugbjerg *et al.* (*22*). This species was covered by hexagonal plates. Another strain (CCMP-2293) had identical small subunit DNA sequences but twice as much DNA as *B. frigida*. It was speculated that this other strain is a diploid stage which, based on the other examples of dimorphism, may have a sheet-like IPC, but this was not examined.

By extrapolation of the four cases of cryptomonads with dimorphic life cycles above, one may speculate that other genera described with a sheet-like periplast not divided into plates, such as *G. cryophila*, *H. phi*, and *Storeatula major*, are likewise diploid stages. Genera with plates include *Cryptomonas*, *Rhodomonas*, *Rhinomonas*, *Chroomonas*, *Komma*, *Falcomonas*, and *Hemiselmis*. Judging from pigmentation, the haploid stage of *Storeatula* may belong to *Rhinomonas*, as suggested by Majaneva *et al.* (*15*), as it resembles *Rhinomonas* in pigmentation and lack of a furrow. The haploid stage of *Geminigera* could perhaps be another species of *Plagioselmis*, since both have three thylakoid lamellae in the chloroplasts. In our phylogenetic analysis, *P. nannoplanctica* clusters together with *G. cryophila*. However, *P. nannoplanctica* is a freshwater species found in the Northern Hemisphere, while *G. cryophila* is a marine species from Antarctica. Thus, they seem unlikely to be two forms of the same life cycle. The haploid stage of *H. phi* may be a yet undiscovered form of the genus *Guillardia*, as the two genera consistently form a clade in molecular trees (*10*).

## Cryptophyte life cycle

In our laboratory cultures, the change from *T. amphioxeia* to *P. prolonga* (meiosis) was observed twice in the Roskilde strains. The change from *P. prolonga* to *T. amphioxeia* (fusion) was never observed in culture, but gamete fusion in cryptophytes has been observed for *Cryptomonas* sp. (*23*, *24*) and *Chroomonas acuta* (*25*). The authors noted that fusion could start when caudal tips of two cells touch, but usually plasmogamy starts when the posterior tip of one cell touches the mid-central region of another cell—that is at the furrow. Notably, the described and putative haploid forms (*P. prolonga* and *B. frigida*) have two cell types, one with a short antapical end and the other with a prolonged antapical end (sometimes called a tail). If one assumes that the process of fusion, as described by Kugrens and Lee (*25*), is universal among cryptophytes, one can speculate that the cells with the tail are "+ cells," and cells with short ends function as "– cells" during the fusion process. The mid-ventral band, as well as the batteries of ejectosomes at the posterior end, might have a function in the fusion process. When studied in thin sections, this antapical area of the *Plagioselmis* stage was found to be packed with ejectosomes (*20*). The mid-ventral band is a feature that has been described for cryptophyte species with plated IPCs (as *P. prolonga*). The band is much less developed or even absent in the *Teleaulax* genus (*16*), similarly to *P. sulcata*, in which the mid-ventral band is featured only in the haplomorph (*12*). Those observations corroborate a potential role of the mid-ventral band during fusion of cells.

## The ecological context of the cryptophyte life stages

Sexual reproduction is common in eukaryotes and likely evolved only once in the last common ancestor to all eukaryotes (*26*). However, for many taxa, sexual reproduction has never been reported, and it is generally assumed that sexual reproduction is more costly than asexual reproduction (*27*). Thus, it is a conundrum as to why sex persists in stable environments where the adaptive advantages of sex are not obvious (*28*). Many single-celled organisms shift to sexual reproduction when starved or stressed (*29*). This could explain why sexual reproduction and life cycle changes are rare under culture conditions and why the trigger from one stage to another has not been determined yet in the laboratory.

Both the haploid *Plagioselmis* stage and the diploid *Teleaulax* stage in this study reproduce mitotically in culture. The life cycle is haplodiplontic, and in contrast to what was believed until recently, the same has now been found to apply to many haptophytes and choanoflagellates (*13*, *30*, *31*). Overall, haplodiplontic life cycles are generalized as an adaptation to a variable environment and would allow a species to occupy more than one niche (*32*). In coccolithophores, haploid and diploid phases are associated with different calcification modes (*13*), and changes in the life phase can be induced depending on the magnitude of stressors (i.e., changes in nutrient and temperature regimes) to which cells are exposed (*33*). In *Phaeocystis globosa*, flagellate cells (haploid) are more prone to grazing but are better competitors for nutrients than the colonial forms (diploid). This correlation is reflected in the distribution patterns of the two morphotypes, with the flagellate form occurring in waters poorer in nutrients than the colonial ones (*31*).

Until now, the interaction between the two life cycle stages of cryptophytes in nature has remained unknown. In natural populations of Roskilde Fjord, both the haploid *Plagioselmis* stage and the diploid *Teleaulax* stage of *T. amphioxeia* are observed year round; however, the relative importance of the two forms changes throughout the year. The diploid form dominates during winter, when DIN concentrations are high and grazing is reduced, while the haploid form increases in relative abundance during late spring and summer, when DIN decreases to potential limiting concentrations and grazing pressure is high [Fig. 1; (*34*)]. Although other factors (i.e., temperature and irradiance) also change during the same period, it is important to highlight that the changes from *T. amphioxeia* to *P. prolonga* observed in cultures occurred in cells kept under constant temperature and light. Therefore, we speculate that either nutrient limitation or an increase in pH due to $CO_2$ limitation could trigger the changes in life cycle stages. Considering that the changes in cultures were observed a while after maximum cell abundances were reached (when pH is the highest), we believe that nutrient depletion was likely more significant than an effect of pH. In addition, the cultures lost their typical reddish coloration, and a reduction of cell size was observed, consistent with previously reported effects of N-limitation on cryptophytes (*35*). In addition to the fact that the relative proportion of haploid and diploid stages in the field did show a significant correlation to DIN but not to DIP (Fig. 1B and fig. S1), evidence suggests that N-limitation could be a trigger for changing life cycle stages in those organisms.

Changes in the predominant life form might be an ecological strategy to cope with resource availability and grazing pressure, as the smaller *Plagioselmis* form has a higher surface-to-volume ratio, optimizing nutrient uptake, and shows a faster growth rate than the diploid form, thus possibly enabling this stage to cope more effectively with intense grazing. The fact that both haploid and diploid populations coexist throughout the year indicates that sexual reproduction might occur frequently. In addition to this work, the co-occurrence of *P. prolonga* and *T. amphioxeia* has been reported in other studies as well. Hill (*36*) reports both forms in all seasons in the western Baltic Sea (Belt Sea and Kattegat), with *P. prolonga* abundant in all seasons except in winter. *T. amphioxeia* was less abundant, but it was also observed in the Gulf of Finland. In the Gulf of Naples, *P. prolonga* was reported as one of the main cryptophyte species, occurring all year round at low cell densities but also, on one occasion, forming a spring bloom (*1*).

The occurrence of *T. amphioxeia* in all seasons might be because of their production of phycobiliproteins (PE545) combined with the haplodiplontic life cycle. Phycobiliproteins function as light-harvesting complexes, capturing light energy and transferring it onto the chlorophylls during photosynthesis (*37*). This allows the organisms to thrive in the temperate winter, when light levels limit the growth of most species. During this time, inorganic nutrients are abundant, and grazing is low (*38*). For *B. frigida*, PE545 (phycoerythrin 545) was produced when cells were exposed to low light intensities, whereas under higher light intensity, the cells were green and did not show the PE545 peak (*22*), illustrating the advantages of PE545 under low light. Furthermore, PE545 is also hypothesized to be a N reservoir, as the molecule is N-rich. When cells are N-limited, PE545 is consumed, causing cells to change color from reddish to a more greenish tone (*35*). We hypothesize that the haplodiplontic life cycle provides the flexibility to endure adversity (nutrient limitation, high grazing, and changes in temperature and light) by changes in cell size and by always ensuring genetic flexibility in the population. This partly explains the species habitat range, spanning over a wide range of temperatures, salinities, and nutrient availability (e.g., Baltic and Mediterranean Sea). The *Plagioselmis* form seems to predominate in nutrient-poor waters (Gulf of Naples; Kattegat) in contrast to areas where inorganic nutrients are seasonally abundant (Roskilde Fjord and Gulf of Finland) and *T. amphioxeia* might be more important. This ecological flexibility could also explain why specialist grazers such as *M. rubrum* rely on *Teleaulax* as prey, which will often be present despite their usually low relative abundance in the natural environment.

We conclude that *P. prolonga* is the haploid life cycle stage of the cryptophyte species *T. amphioxeia* and should thus be referred to as the *Plagioselmis* stage of *T. amphioxeia*. We determined the two taxa to be the same species because of a change of morphology in culture and congruent 18*S* rDNA sequences. We conclude that one is the haploid form of the other because the *Plagioselmis* stage contains half the DNA of *T. amphioxeia*. As more dimorphisms are found in both known and still-undescribed species, future studies are likely to synonymize more species. The frequency and role of sexual reproduction in protists remain enigmatic, especially in natural environments. Here, we provide an ecological perspective to the change between forms. The dimorphic life cycle of *T. amphioxeia* may explain its persistence and success, as the smaller haploid form appears to dominate during periods of increased grazing pressure and lower nutrients. In future studies, ecological perspectives like the one presented here may provide valuable knowledge on the frequency and role of sexual reproduction in protists in their natural environments, something that is presently poorly understood.

## MATERIALS AND METHODS

### Experimental design

Environmental water samples (2 liters) were taken approximately daily between February 2016 and November 2017 at the surface of a fixed station (55°41′30.19″N, 12°04′55.24″E) located in Roskilde Fjord, Denmark. Samples were brought to the laboratory shortly after sampling (10 to 20 min.), where live samples of phytoplankton were analyzed by a pulse-recording flow cytometer CytoSense (CytoBuoy, The Netherlands). Samples were also analyzed weekly for DIN and DIP ($PO_4^{3-}$) on a Scan++ Continuous Flow Analyzer (Skalar Analytical B.V., Breda, The Netherlands) following the methodology described in (*39*). DIN was calculated as the sum of measured $NO_2^-$, $NO_3^-$, and $NH_4^+$.

For phytoplankton enumeration, 500 to 1000 µl of live samples were analyzed with CytoSense [at a flow rate of 8 µl $s^{-1}$ and a trigger level of 30 mV for the FLR (red fluorescence) sensor]. For each particle, signals are acquired from multiple detectors as the particle or cell travels through the laser beam focus, originating an optical profile. Optical profiles were obtained by the software CytoUSB (cytobuoy.com) and used to identify populations with similar optical properties (clusters). Here, we focused on the cryptophyte clusters [characterized by high orange fluorescence (FLO) relative to FLR] identified as *T. amphioxeia* and *P. prolonga*. They were further distinguished from each other by lower intensities of FLR, FLO, and FWS (forward scatter, indicating smaller size) of *P. prolonga* compared to *T. amphioxeia* and by their distinct optical profile shapes: a pronounced shoulder on the scattering signal for *T. amphioxeia* while more regular in *P. prolonga* (fig. S3). Identification of the clusters was confirmed by pictures taken by CytoSense and by periodic sample observation in the light microscope.

In those samples, cryptophytes were always present and dominated total phytoplankton biomass in different periods (*34*). Cultures were established for species identification. For one *T. amphioxeia* isolate, a change in morphology was observed when cultures were left undisturbed for an extended period (approximately 1.5 months), with cells losing the characteristic reddish coloration, decreasing in size, and becoming more rounded. After culture replication, cells recovered their typical color and hyaline tail but did not recover in size. After close inspection under the light microscope, it was confirmed that the morphology had changed from *T. amphioxeia* to *P. prolonga*. Life form change in our cultures was also indicated by an increase in growth rates, as under the same conditions, *P. prolonga* cultures needed to be transferred more often than *T. amphioxeia*. In addition, *P. prolonga* cultures sustained higher cell densities without signs of stress (i.e., change in coloration) for longer periods than *T. amphioxeia*. The life form change was observed twice, indicating that *T. amphioxeia* and *P. prolonga* are not two distinct species but different life cycle stages of the same species. This potential dimorphism was verified by sequencing of rDNA and investigating cell morphology and ploidy. Detailed information on the methods used for DNA extraction, polymerase chain reaction, sequencing, ploidy determination and morphology studies, and CytoSense specifications can be found in Table 1, Supplementary Materials and Methods, and table S2.

### Statistical analysis

To examine the hypothesized relationship of life-cycle stage to DIN, a semi-parametric GAM was used to determine the abundance ratio between *P. prolonga* and *T. amphioxeia* (*40*). The GAM included a linear relationship to DIN and a nonparametric smoother for the

**Table 1. Accession numbers of newly sequenced strains.**

| Species | Strain | Gene | Length (bp) | Accession number |
|---|---|---|---|---|
| ***Teleaulax amphioxeia*** | SCCAP:K-1837 | 18*S* partial | 1218 | MK956825 |
| | | ITS1, 5.8*S*, ITS2 | 648 | MT420722 |
| ***Teleaulax amphioxeia*** | Roskilde March | 18*S* partial | 1651 | MK956196 |
| ***Plagioselmis prolonga*** | Roskilde December | 18*S* partial | 1173 | MK956143 |
| | | ITS1, 5.8*S*, ITS2 | 726 | MT420721 |
| ***Teleaulax acuta*** | SCCAP:K-1486 | 18*S* partial | 1201 | MK956814 |
| ***Geminigera cryophila*** | RCC5152 | 18*S* partial | 1745 | MK956818 |
| ***Teleaulax amphioxeia*** | SCCAP:K-0434 | 5.8*S* partial, ITS2, 28*S* partial | 687 | JN584173 |

departure from this relationship over time. For visualizing the time trajectory, a smoothed version of the DIN time trend was scored with the GAM. Both DIN and abundance ratios were log-transformed before analysis to address the inherent scale dependency in the data, and results from the GAM approach were back-transformed for visualization. Note that only data on cell abundances (cells per milliliter), rather than biomass, were compared in this study, as the larger size of *T. amphioxeia* would inflate their relative importance and mask dynamics of *P. prolonga*.

## SUPPLEMENTARY MATERIALS

Supplementary material for this article is available at http://advances.sciencemag.org/cgi/content/full/6/37/eabb1611/DC1

## REFERENCES AND NOTES


1. F. Cerino, A. Zingone, A survey of cryptomonad diversity and seasonality at a coastal Mediterranean site. *Eur. J. Phycol.* **41**, 363–378 (2006).
2. D. E. Gustafson, D. K. Stoecker, M. D. Johnson, W. F. Van Heukelem, K. Sneider, Cryptophyte algae are robbed of their organelles by the marine ciliate *Mesodinium rubrum*. *Nature* **405**, 1049–1052 (2000).
3. P. J. Hansen, M. Moldrup, W. Tarangkoon, L. Garcia-Cuetos, Ø. Moestrup, Direct evidence for symbiont sequestration in the marine red tide ciliate *Mesodinium rubrum*. *Aquat. Microb. Ecol.* **66**, 63–75 (2012).
4. K. Koike, K. Takishita, Anucleated cryptophyte vestiges in the gonyaulacalean dinoflagellates *Amylax buxus* and *Amylax triacantha* (Dinophyceae). *Phycol. Res.* **56**, 301–311 (2008).
5. M. G. Park, M. Kim, M. Kang, A dinoflagellate *Amylax triacantha* with plastids of the cryptophyte origin: phylogeny, feeding mechanism, and growth and grazing responses. *J. Eukaryot. Microbiol.* **60**, 363–376 (2013).
6. P. J. Hansen, L. T. Nielsen, M. Johnson, T. Berge, K. J. Flynn, Acquired phototrophy in *Mesodinium* and *Dinophysis* - A review of cellular organization, prey selectivity, nutrient uptake and bioenergetics. *Harmful Algae* **28**, 126–139 (2013).
7. E. Peltomaa, M. D. Johnson, *Mesodinium rubrum* exhibits genus-level but not species-level cryptophyte prey selection. *Aquat. Microb. Ecol.* **78**, 147–159 (2017).
8. P. Rial, A. Laza-Martinez, B. Reguera, N. Raho, F. Rodriguez, Origin of cryptophyte plastids in *Dinophysis* from Galician waters: results from field and culture experiments. *Aquat. Microb. Ecol.* **76**, 163–174 (2015).
9. B. L. Clay, P. Kugrens, R. E. Lee, A revised classification of Cryptophyta. *Bot. J. Linn. Soc.* **131**, 131–151 (1999).
10. K. Hoef-Emden, B. Marin, M. Melkonian, Nuclear and nucleomorph SSU rDNA phylogeny in the Cryptophyta and the evolution of cryptophyte diversity. *J. Mol. Evol.* **55**, 161–179 (2002).
11. K. Hoef-Emden, Molecular phylogeny of phycocyanin-containing cryptophytes: Evolution of biliproteins and geographical distribution. *J. Phycol.* **44**, 985–993 (2008).
12. D. R. A. Hill, R. Wetherbee, *Proteomonas sulcata* gen. et sp. nov. (Cryptophyceae), a cryptomonad with two morphologically distinct and alternating forms. *Phycologia* **25**, 521–543 (1986).
13. A. Houdan, C. Billard, D. Marie, F. Not, A. G. Sáez, J. R. Young, I. Probert, Holococcolithophore-heterococcolithophore (Haptophyta) life cycles: Flow cytometric analysis of relative ploidy levels. *Syst. Biodivers.* **1**, 453–465 (2004).
14. K. Hoef-Emden, M. Melkonian, Revision of the genus *Cryptomonas* (Cryptophyceae): a combination of molecular phylogeny and morphology provides insights into a long-hidden dimorphism. *Protist* **154**, 371–409 (2003).
15. M. Majaneva, I. Remonen, J.-M. Rintala, I. Belevich, A. Kremp, O. Setälä, E. Jokitalo, J. Blomster, *Rhinomonas nottbecki* n. sp. (Cryptomonadales) and molecular phylogeny of the family Pyrenomonadaceae. *J. Eukaryot. Microbiol.* **61**, 480–492 (2014).
16. A. Laza-Martinez, J. Arluzea, I. Miguel, E. Orive, Morphological and molecular characterization of *Teleaulax gracilis* sp. nov. and *T. minuta* sp. nov. (Cryptophyceae). *Phycologia* **51**, 649–661 (2012).
17. R. W. Butcher, An introductory account of the smaller algae of British coastal waters. Part IV: Cryptophyceae, in *Fishery Investigations, Series IV* (Her Majesty's Stationery Office, 1967), pp. 1–54.
18. N. J. Turland et al., *International Code of Nomenclature for algae, fungi, and plants (Shenzhen Code) adopted by the Nineteenth International Botanical Congress Shenzhen, China, July 2017* (Koeltz Botanical Books, Glashütten, 2018).
19. M.-J. Chrétiennot-Dinet, *Chlorarachnophycées, Chlorophycées, Chrysophycées, Cryptophycées, Euglénophycées, Eustigmatophycées, Prasinophycées, Prymnesiophycées, Rhodophycées et Tribophycées* (Atlas du phytoplancton marin, Éditions du CNRS, 1990) vol. 3.
20. G. Novarino, I. A. N. Lucas, S. Morrall, Observations on the genus *Plagioselmis* (Cryptophyceae). *Cryptogam. Algol.* **15**, 87–107 (1994).
21. D. R. A. Hill, A revised circumscription of *Cryptomonas* (Cryptophyceae) based on examination of Australian strains. *Phycologia* **30**, 170–188 (1991).
22. N. Daugbjerg, A. Norlin, C. Lovejoy, *Baffinella frigidus* gen. et sp. nov. (Baffinellaceae fam. nov., Cryptophyceae) from Baffin Bay: Morphology, pigment profile, phylogeny, and growth rate response to three abiotic factors. *J. Phycol.* **54**, 665–680 (2018).
23. F. Wawrik, Sexualität bei *Cryptomonas* sp. und *Chlorogonium maximum*. *Nova Hedwigia* **8**, 283–292 (1969).
24. F. Wawrik, Eisschluß- und Eisbruchvegetationen in den Teichen des nördlichen Waldviertels 1977/1978. *Arch. Protistenkd.* **122**, 247–266 (1979).
25. P. Kugrens, R. E. Lee, Ultrastructure of fertilization in a cryptomonad. *J. Phycol.* **24**, 385–393 (1988).
26. U. Goodenough, J. Heitman, Origins of eukaryotic sexual reproduction. *Cold Spring Harb. Perspect. Biol.* **6**, a016154 (2014).
27. D. Speijer, J. Lukes, M. Elias, Sex is a ubiquitous, ancient, and inherent attribute of eukaryotic life. *Proc. Natl. Acad. Sci. U.S.A.* **112**, 8827–8834 (2015).
28. M. Brandeis, New-age ideas about age-old sex: separating meiosis from mating could solve a century-old conundrum. *Biol. Rev.* **93**, 801–810 (2018).
29. Y. Ram, L. Hadany, Condition-dependent sex: who does it, when and why? *Philos. Trans. R. Soc. B* **371**, 1–8 (2016).
30. H. A. Thomsen, J. B. Østergaard, Circumstantial evidence of life history events in loricate choanoflagellates. *Eur. J. Protistol.* **58**, 26–34 (2017).
31. L. Peperzak, F. Colijn, E. G. Vrieling, W. W. C. Gieskes, J. C. H. Peeters, Observations of flagellates in colonies of *Phaeocystis globosa* (Prymnesiophyceae); a hypothesis for their position in the life cycle. *J. Plankton Res.* **22**, 2181–2203 (2000).
32. M. Valero, S. Richerd, V. Perrot, C. Destombe, Evolution of alternation of haploid and diploid phases in life cycles. *Trends Ecol. Evol.* **7**, 25–29 (1992).
33. M.-H. Nöel, M. Kawachi, I. Inouye, Induced Dimorphic Life Cycle of a Coccolithophorid, *Calyptrosphaera sphaeroidea* (Prymnesiophyceae, Haptophyta). *J. Phycol.* **40**, 112–129 (2004).
34. L. Haraguchi, H. H. Jakobsen, N. Lundholm, J. Carstensen, Phytoplankton community dynamic: A driver for ciliate trophic strategies. *Front. Mar. Sci.* **5**, 1–16 (2018).

35. A. J. Lewitus, D. A. Caron, Relative effects of nitrogen or phosphorus depletion and light intensity on the pigmentation, chemical composition, and volume of *Pyrenomonas salina* (Cryptophyceae). *Mar. Ecol. Prog. Ser.* **61**, 171–181 (1990).
36. D. R. A. Hill, *Teleaulax amphioxeia* Conrad (Hill), comb. nov. (Cryptophyceae). Baltic Sea Identification Sheet No. 13. *Ann. Bot. Fennici.*, 175–176 (1992).
37. L. Spear-Bernstein, K. R. Miller, Unique location of the phycobiliprotein light-harvesting pigment in the Cryptophyceae. *J. Phycol.* **25**, 412–419 (1989).
38. B. Walter, J. Peters, J. E. E. van Beusekom, The effect of constant darkness and short light periods on the survival and physiological fitness of two phytoplankton species and their growth potential after re-illumination. *Aquat. Ecol.* **51**, 591–603 (2017).
39. K. Grasshof, *Methods of Seawater Analysis* (Verlag Chemie, 1976).
40. J. Carstensen, in *Application of Threshold Concepts in Natural Resource Decision Making*, G. R. Guntenspergen, Ed. (Springer, 2014), pp. 255–272.
41. A. R. Loeblich III, V. E. Smith, Chloroplast pigments of the marine dinoflagellate *Gyrodinium resplendens*. *Lipids* **3**, 5–13 (1968).
42. M. L. Richlen, P. H. Barber, A technique for the rapid extraction of microalgal DNA from single live and preserved cells. *Mol. Ecol. Notes* **5**, 688–691 (2005).
43. G. Landan, D. Graur, Local reliability measures from sets of co-optimal multiple sequence alignments. *Pac. Symp. Biocomput.* **13**, 15–24 (2008).
44. I. Sela, H. Ashkenazy, K. Katoh, T. Pupko, GUIDANCE2: accurate detection of unreliable alignment regions accounting for the uncertainty of multiple parameters. *Nucleic Acids Res.* **43**, W7–W14 (2015).
45. S. Guindon, J.-F. Dufayard, V. Lefort, M. Anisimova, W. Hordijk, O. Gascuel, New algorithms and methods to estimate maximum-likelihood phylogenies: assessing the performance of PhyML 3.0. *Syst. Biol.* **59**, 307–321 (2010).
46. V. Lefort, J. E. Longueville, O. Gascuel, SMS: Smart Model Selection in PhyML. *Mol. Biol. Evol.* **34**, 2422–2424 (2017).
47. J. P. Huelsenbeck, F. Ronquist, MRBAYES: Bayesian inference of phylogenetic trees. *Bioinformatics* **17**, 754–755 (2001).
48. A. Nabbi, K. Riabowol, Rapid isolation of nuclei from cells in vitro. *Cold Spring Harb Protoc* **2015**, 769–772 (2015).
49. D. Marie, F. Partensky, S. Jacquet, D. Vaulot, Enumeration and cell cycle analysis of natural populations of marine picoplankton by flow cytometry using the nucleic acid stain SYBR Green I. *Appl. Environ. Microbiol.* **63**, 186–193 (1997).
50. G. B. Dubelaar, P. J. Geerders, R. R. Jonker, High frequency monitoring reveals phytoplankton dynamics. *J. Environ. Monit.* **6**, 946–952 (2004).
51. M. Thyssen, S. Alvain, A. Lefèbvre, D. Dessailly, M. Rijkeboer, N. Guiselin, V. Creach, L.-F. Artigas, High-resolution analysis of a North Sea phytoplankton community structure based on in situ flow cytometry observations and potential implication for remote sensing. *Biogeosciences* **12**, 4051–4066 (2015).
52. Y. Takano, T. Horiguchi, Surface ultrastructure and molecular phylogenetics of four unarmored heterotrophic dinoflagellates, including the type species of the genus *Gyrodinium* (Dinophyceae). *Phycol. Res.* **52**, 107–116 (2004).
53. T. J. White, T. Bruns, S. Lee, J. Taylor, in *PCR Protocols: A Guide to Methods and Applications*, M. A. Innis, J. J. Gelfand, J. J. Sninsky, T. J. White, Eds. (Academic Press, 1990), pp. 315–322.
54. A. Yamaguchi, T. Horiguchi, Molecular phylogenetic study of the heterotrophic dinoflagellate genus *Protoperidinium* (Dinophyceae) inferred from small subunit rRNA gene sequences. *Phycol. Res.* **53**, 30–42 (2005).
55. L. Medlin, H. J. Elwood, S. Stickel, M. L. Sogin, The characterization of enzymatically amplified eukaryotic 16S-like rRNA-coding regions. *Gene* **71**, 491–499 (1988).



**Acknowledgments**

**Funding:** L.H. was supported by a grant from the Brazilian program Science without Borders/CAPES (grant no. 13581-13-9). This study is a contribution from the BONUS COCOA project (grant agreement 2112932-1) supported by Innovation Fund Denmark and the European Union. A.A., N.L., and P.J.H. were supported by a grant from The Danish Council for Independent Research to P.J.H. (grant no. 4181-00484). The publication charges for this article have been funded by a grant from the publication fund of UiT The Arctic University of Norway. N.L. acknowledges support from the Villum Foundation under grant no. 00023065. **Author contributions:** L.H. and A.A. conceived the taxonomical part of the study; J.C., H.H.J., and L.H. conceived the ecological part of the study. H.E.B., L.H., and A.A. did molecular work; L.H., L.G.-C, and Ø.M. performed SEM. A.A., L.H., and H.E.B. drafted the manuscript. All authors contributed to writing the manuscript and read and approved the final version of the manuscript. **Competing interests:** The authors declare that they have no competing interests. **Data and materials availability:** All data needed to evaluate the conclusions in the paper are present in the paper and/or the Supplementary Materials. Additional data related to this paper may be requested from the authors.

Submitted 6 February 2020
Accepted 29 July 2020
Published 11 September 2020
10.1126/sciadv.abb1611

**Citation:** A. Altenburger, H. E. Blossom, L. Garcia-Cuetos, H. H. Jakobsen, J. Carstensen, N. Lundholm, P. J. Hansen, Ø. Moestrup, L. Haraguchi, Dimorphism in cryptophytes—The case of *Teleaulax amphioxeia*/*Plagioselmis prolonga* and its ecological implications. *Sci. Adv.* **6**, eabb1611 (2020).

Science Advances

# Dimorphism in cryptophytes—The case of *Teleaulax amphioxeia*/*Plagioselmis prolonga* and its ecological implications

A. Altenburger, H. E. Blossom, L. Garcia-Cuetos, H. H. Jakobsen, J. Carstensen, N. Lundholm, P. J. Hansen, Ø. Moestrup and L. Haraguchi

*Sci Adv* **6** (37), eabb1611.
DOI: 10.1126/sciadv.abb1611